US 20120295027A1

(19) **United States**

(12) **Patent Application Publication**

Liu et al.

(10) **Pub. No.: US 2012/0295027 A1**

(43) **Pub. Date: Nov. 22, 2012**

(54) **MESOPOROUS METAL OXIDE GRAPHENE NANOCOMPOSITE MATERIALS**

(75) Inventors: **Jun Liu**, Richland, WA (US); **Ilhan A. Aksay**, Princeton, NJ (US); **Rong Kou**, Richland, WA (US); **Donghai Wang**, State College, PA (US)

(73) Assignee: **Battelle Memorial Institute and The Trustees of Princeton University**

(21) Appl. No.: **13/559,538**

(22) Filed: **Jul. 26, 2012**

Related U.S. Application Data

(62) Division of application No. 12/553,527, filed on Sep. 3, 2009.

(60) Provisional application No. 61/095,421, filed on Sep. 9, 2008, provisional application No. 61/099,388, filed on Sep. 23, 2008.

Publication Classification

(51) **Int. Cl.**

B05D 5/00 (2006.01)

B82Y 40/00 (2011.01)

(52) **U.S. Cl.** **427/245**; 977/890

(57) **ABSTRACT**

A nanocomposite material formed of graphene and a mesoporous metal oxide having a demonstrated specific capacity of more than 200 F/g with particular utility when employed in supercapacitor applications. A method for making these nanocomposite materials by first forming a mixture of graphene, a surfactant, and a metal oxide precursor, precipitating the metal oxide precursor with the surfactant from the mixture to form a mesoporous metal oxide. The mesoporous metal oxide is then deposited onto a surface of the graphene.

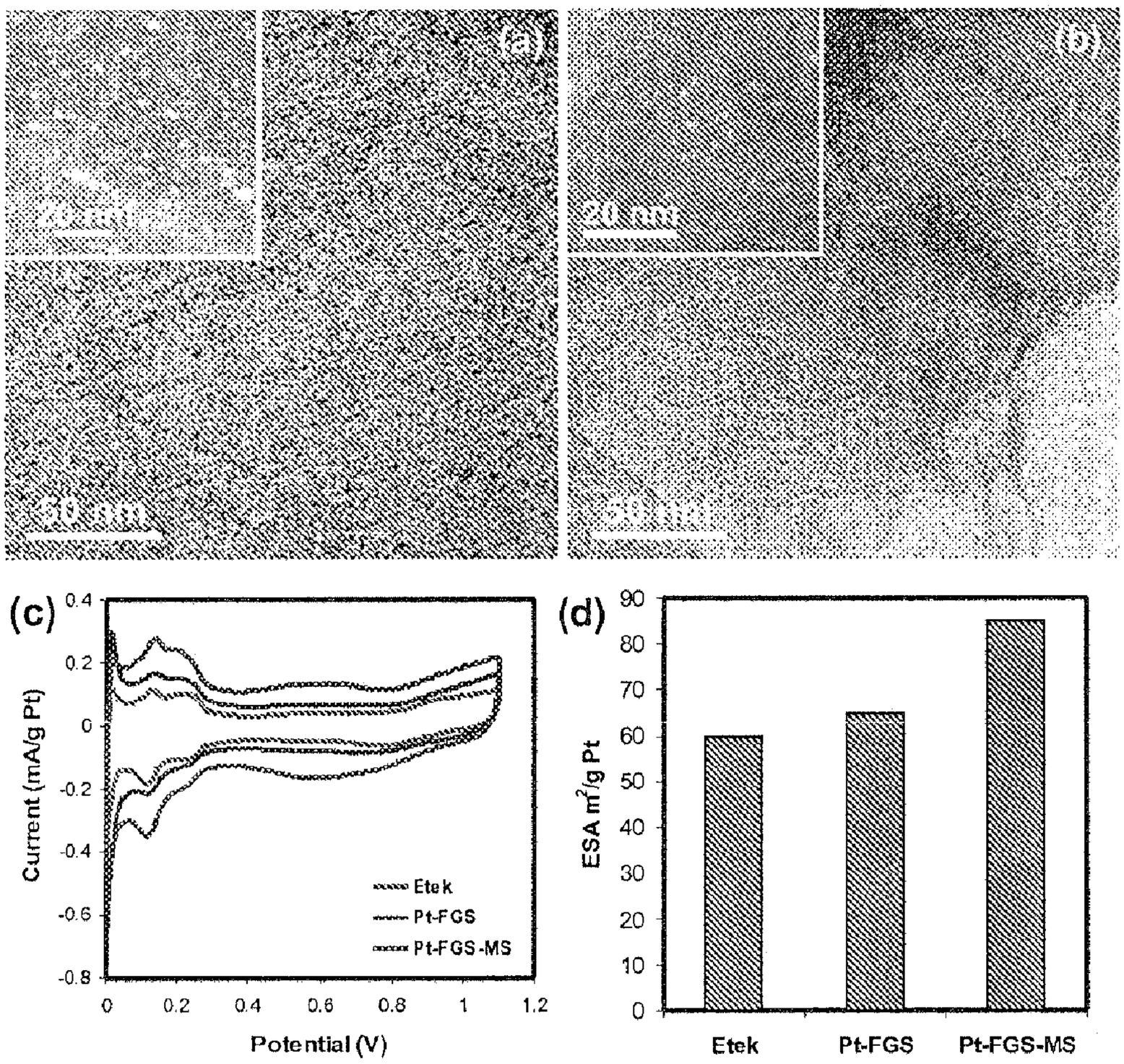

Figure 1

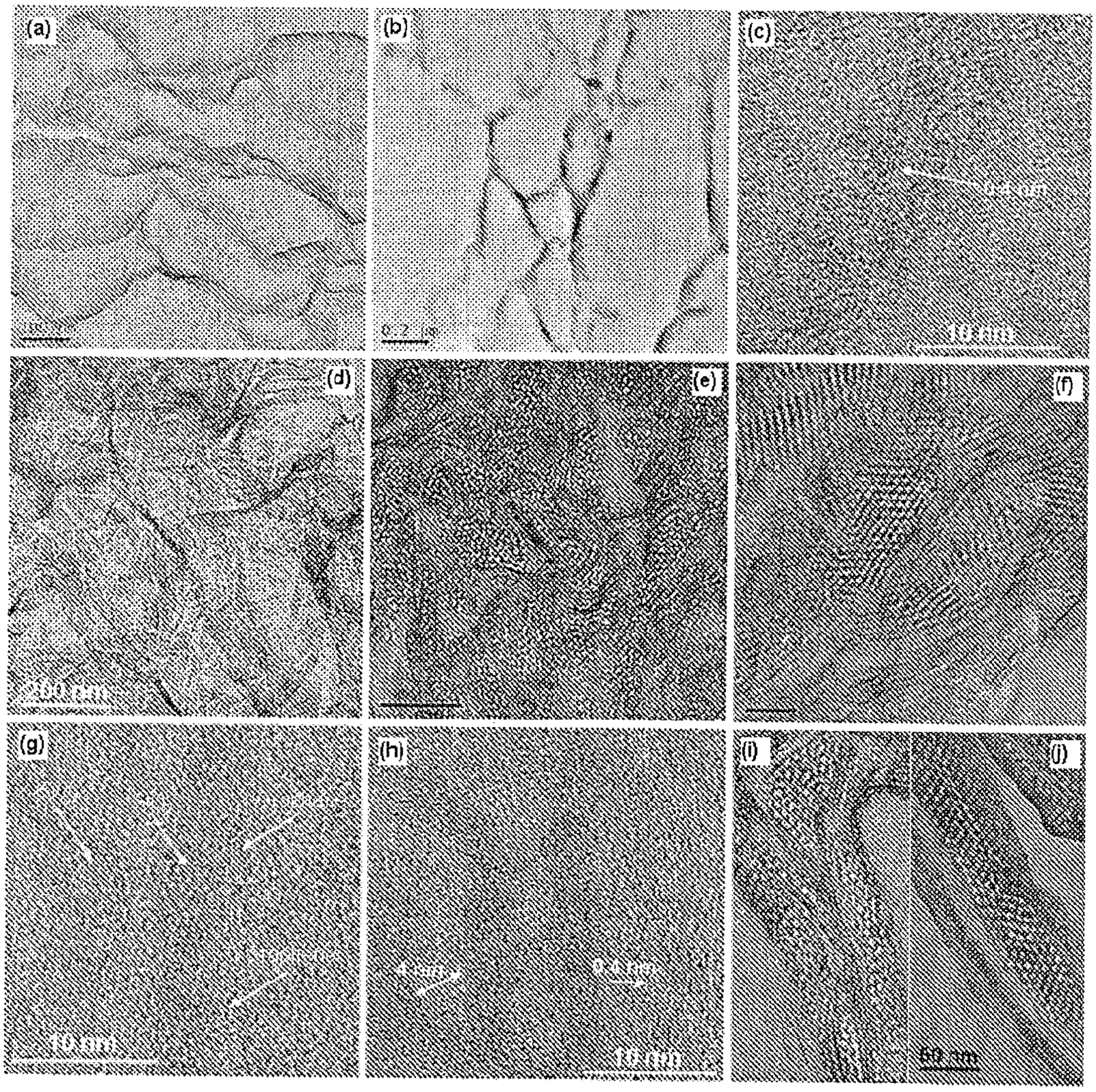

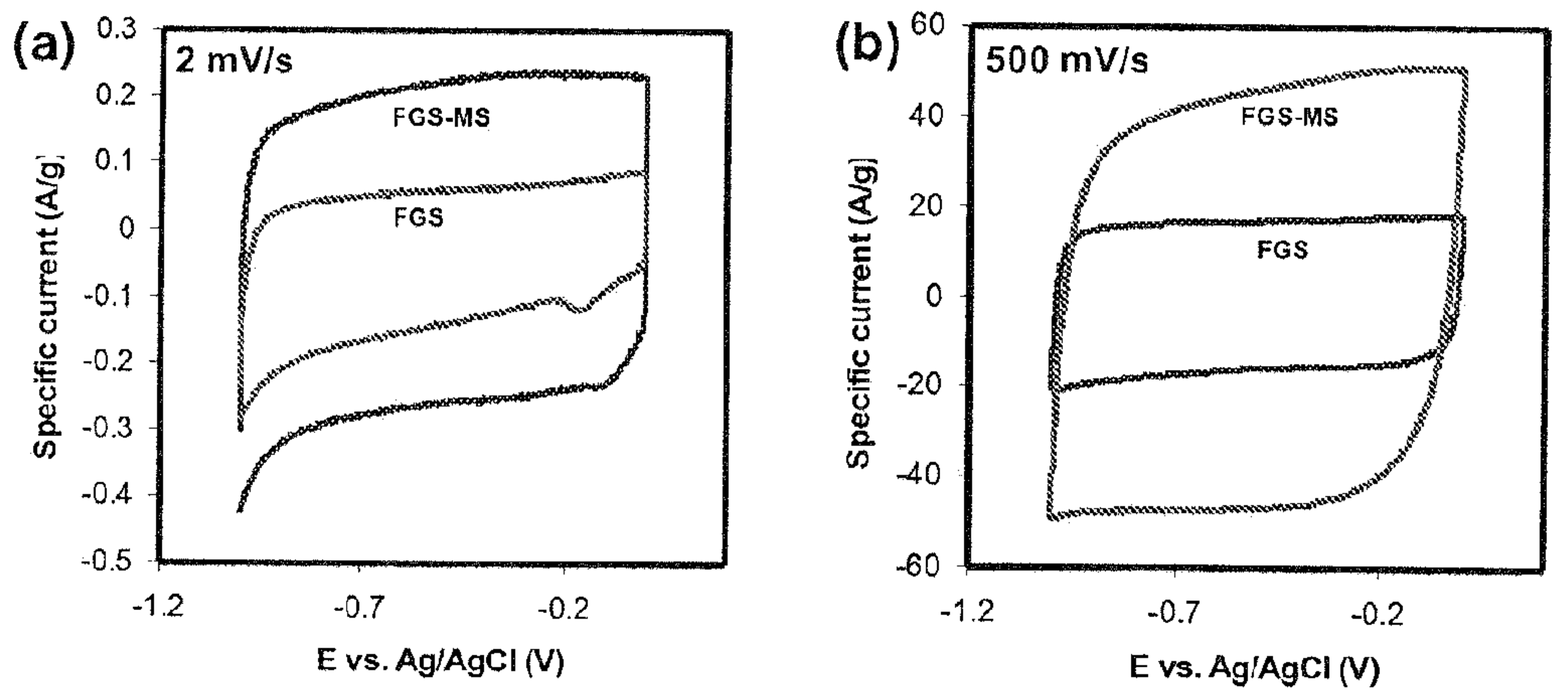
(a)
2 mV/s
FGS-MS
FGS
Specific current (A/g)
0.3
0.2
0.1
0
-0.1
-0.2
-0.3
-0.4
-0.5
-1.2
-0.7
-0.2
E vs. Ag/AgCl (V)
(b)
500 mV/s
FGS-MS
FGS
Specific current (A/g)
60
40
20
0
-20
-40
-60
-1.2
-0.7
-0.2
E vs. Ag/AgCl (V)

Figure 2.

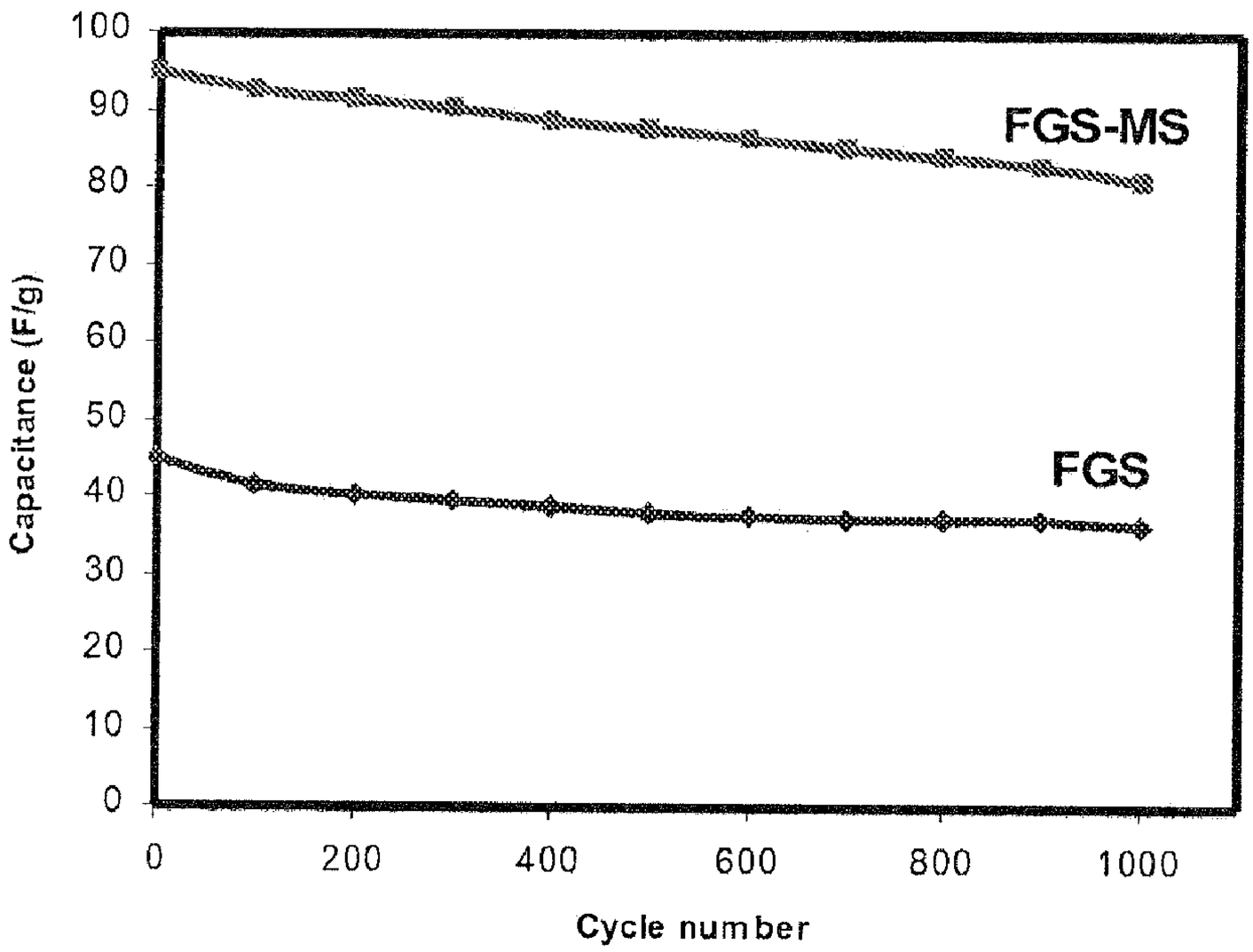
100
90
80
70
60
50
40
30
20
10
0
Capacitance (F/g)
FGS-MS
FGS
0
200
400
600
800
1000
Cycle number

Figure 3

Figure 4.

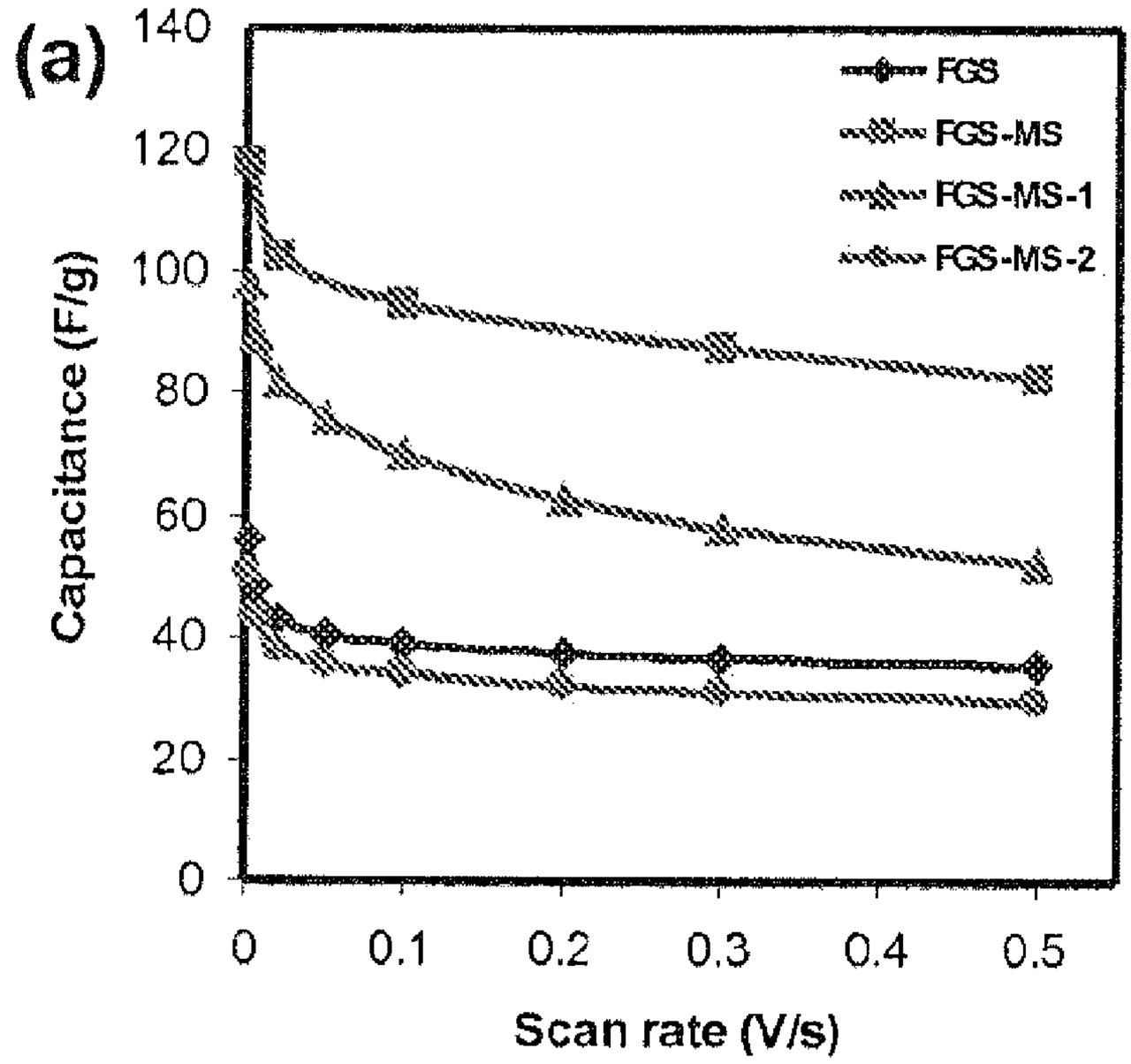
(a)
140
120
100
80
60
40
20
0
Capacitance (F/g)
FGS
FGS-MS
FGS-MS-1
FGS-MS-2
0
0.1
0.2
0.3
0.4
0.5
Scan rate (V/s)

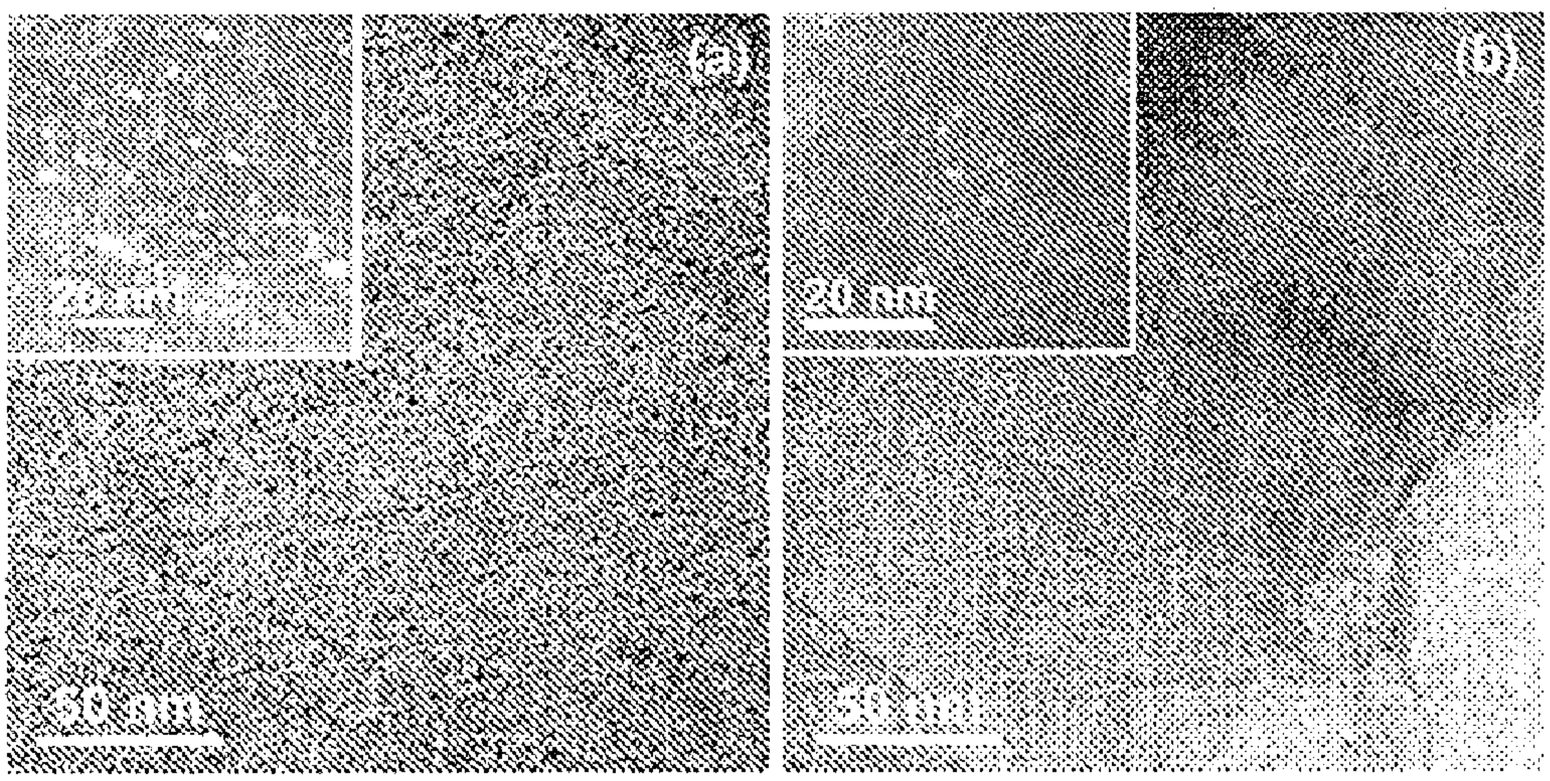
(a)
20 nm
(b)
20 nm

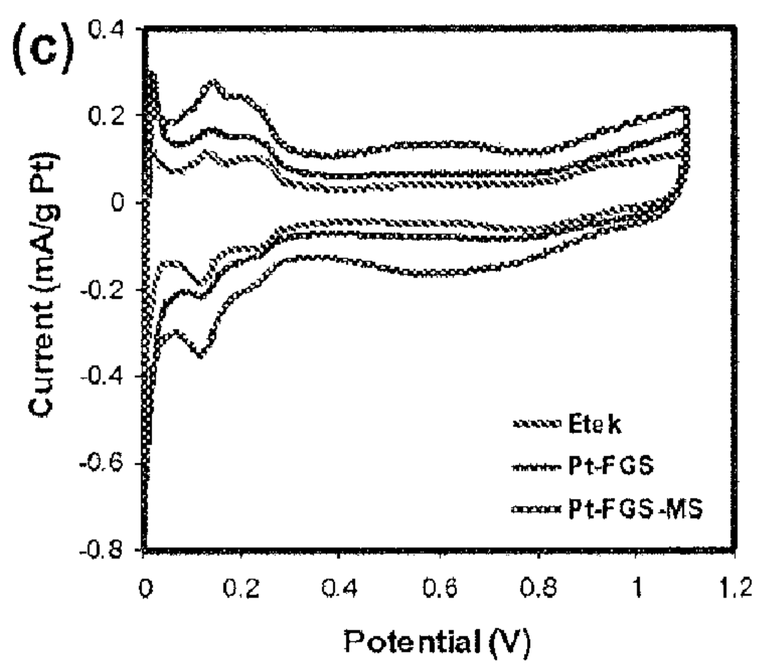
(c)
Current (mA/g Pt)
0.4
0.2
0
-0.2
-0.4
-0.6
-0.8
0
0.2
0.4
0.6
0.8
1
1.2
Potential (V)
Etek
Pt-FGS
Pt-FGS-MS

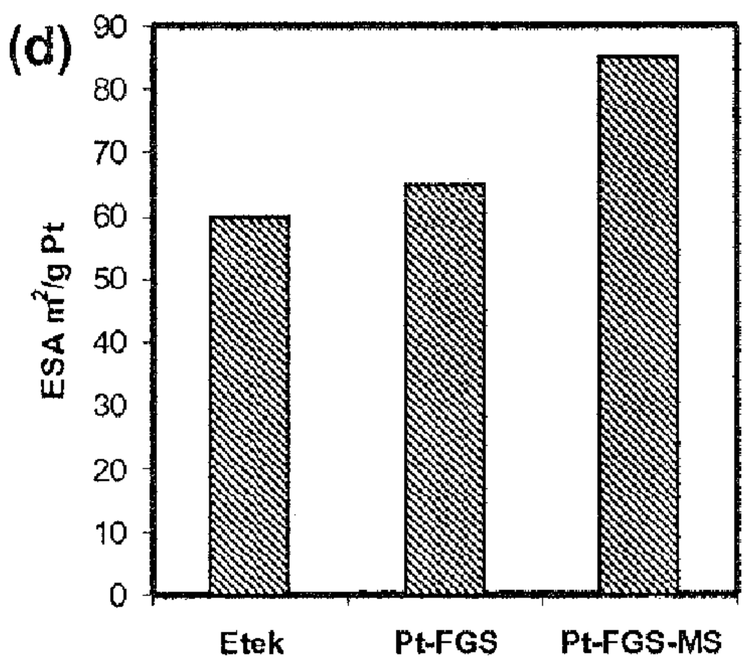
(d)
ESA m²/g Pt
90
80
70
60
50
40
30
20
10
0
Etek
Pt-FGS
Pt-FGS-MS

Figure 5

MESOPOROUS METAL OXIDE GRAPHENE NANOCOMPOSITE MATERIALS

PRIORITY CLAIM

[0001] This application claims priority from provisional patent application No. 61/095,421, filed Sep. 9, 2008 as well as provisional patent application No. 61/099,388 filed Sep. 23, 2008 the contents of both are herein incorporated by reference.

[0002] The invention was made with Government support under Contract DE-AC0676RLO 1830, awarded by the U.S. Department of Energy. The Government has certain rights in the invention.

TECHNICAL FIELD

[0003] This invention relates to improved materials used in electrochemical applications such as batteries, capacitors and supercapacitors. More specifically, the present invention relates to nanocomposite materials combining mesoporous metal oxides and graphene which exhibit electrical properties heretofore unknown in the art.

BACKGROUND OF THE INVENTION

[0004] Recent studies have focused on the development of ultracapacitors (or supercapacitors) as advanced electrical energy storage devices to increase the efficiency of energy utilization. In most commercial ultracapacitor applications, high surface area carbon has become the leading candidate material in the development of electrochemical ultracapacitors. These devices are also referred to as electrochemical double layer capacitors (EDLC) since the basic mechanism of electrical energy storage is through charge separation in the electrochemical double layer formed at the electrode/electrolyte interfacial regions. When the electrode is biased, a double layer structure is developed with the opposite charge accumulated near the electrode surface. The double layer thickness (d) is related to the Debye screening length in the modified Gouy-Chapman model. The double layer capacitance (c) is related to the surface area, the effective dielectric constant (ϵ) and the double layer thickness by an inverse linear relationship ($C=\epsilon A/d$). A typical smooth surface will have a double layer capacitance of about 10-20 μF/cm2. In order to enhance mass storage density, high surface area electrodes are necessary. Thus, for a conducting material with a specific surface area of 1000 m^2/g, the capacitance can be increased to 100 F/g.

[0005] In most commercial applications, high surface area carbon-based materials have been the material of choice mainly due to their high electronic conductivity and availability at modest cost. A wide range of high surface area carbon-based materials have been investigated, including activated carbon, multi- and single walled carbon nanotubes. The capacitance typically ranges from 40 to 140 F/g for activated carbon, and 15 to 135 F/g for carbon nanotubes. Currently, the best available commercial products reach about 130 F/g.

[0006] Those active in the art have pursued several approaches toward improving the charge storage density in carbon-based supercapacitors. These approaches have typically focused on achieving a higher capacitance either by careful thermal, chemical, or electrochemical treatment of the carbon-based material to increase the accessible surface area and surface functional groups, or by extending the operating voltage range beyond the limit of an aqueous electrolyte solution.

[0007] Pursuing the first approach, significant effort has been made to maximize the surface area of carbon-based materials. Pursuing the second approach, significant effort has been made to increase the capacitance by modifying the interface. For example, surface functionalization proves to be effective in increasing the pseudocapacitance arising from oxidation/reduction of surface quindoidal functional groups generated during sample treatment. Another widely investigated method enhances the capacitance by coating the carbon-based material with redox active metal oxides such as manganese oxides or conducting polymers such as polyaniline and polypyrrole. With this method, polypyrrole coated carbon nanotubes have been shown to attain a capacitance of 170 F/g, and MnO_2 coated carbon nanotubes have been shown to attain a capacitance of 140 F/g, but these composite materials still do not offset the fundamental limitations of the polymer and MnO_2, including limited stability and operating voltage range.

[0008] Because optimization through surface area and extending the operating voltage range beyond the limit of an aqueous electrolyte solution cannot result in further major improvements, fundamentally new mechanisms need to be discovered to achieve the next significant jump in the storage density of ultracapacitors. The present invention provides one such new mechanism.

[0009] Recently, graphene, highly dispersed atom-layer of hexagonal arrayed carbon atoms, has attracted the interest of those seeking to fabricate new composite materials for molecular electronics due to its high conductivity and good mechanical properties. The combination of high electrical conductivity, good mechanical properties, high surface area, and low manufacturing cost make graphene an ideal candidate material for electrochemical applications. Assuming an active surface area of 2600 m'/g and typical capacitance of 10 $\mu F/m^2$ for carbon materials, graphene has the potential to reach 260 F/g in theoretical specific capacity. However, this high capacity has not been reached because it has proven difficult to completely disperse the graphene sheets and the access all the surface area.

[0010] Graphene is generally described as a one-atom-thick planar sheet of sp^2-bonded carbon atoms that arc densely packed in a honeycomb crystal lattice. The carbon-carbon bond length in graphene is approximately 0.142 nm. Graphene is the basic structural element of some carbon allotropes including graphite, carbon nanotubes and fullerenes. Graphene exhibits unique properties, such as very high strength and very high conductivity.

[0011] Graphene has been produced by a variety of techniques. For example, graphene is produced by the chemical reduction of graphene oxide, as shown in Gomez-Navarro, C.; Weitz, R. T.; Bittner, A. M.; Scolari, M.; Mews, A.; Burghard, M.; Kern, K. Electronic Transport Properties of Individual Chemically Reduced Graphene Oxide Sheets. and *Nano Lett.* 2007, 7, 3499-3503.Si, Y.; Samulski, E. T. Synthesis of Water Soluble Graphenc. *Nano Lett.* 2008, 8, 1679-1682.

[0012] While the resultant product shown in the forgoing methods is generally described as graphene, it is clear from the specific capacity of these materials that complete reduction is not achieved, because the resultant materials do not approach the theoretical specific capacity of neat graphene.

Accordingly, at least a portion of the graphene is not reduced, and the resultant material contains at least some graphene oxide. As used herein, the term "graphene" should be understood to encompass materials such as these, that contain both graphene and small amounts of graphene oxide.

[0013] For example, functionalized graphene sheets (FGSs) prepared through the thermal expansion of graphite oxide as shown in McAllister, M. J.; LiO, J. L.; Adamson, D. H.; Schnicpp, H. C.; Abdala, A. A.; Liu, J.; Herrera-Alonso, M.; Milius, D. L.; CarO, R.; Prud'homme, R. K.; Aksay, I. A. Single Sheet Functionalized Graphene by Oxidation and Thermal Expansion of Graphite. *Chem. Mater.* 2007, 19, 4396-4404 and Schniepp, H. C.; Li, J. L.; McAllister, M. J.; Sai, H.; Herrera-Alonso, M.; Adamson, D. H.; Prud'homme, R. K.; Car, R.; Saville, D. A.; Aksay, I. A. Functionalized Single Graphene Sheets Derived from Splitting Graphite Oxide. *J. Phys. Chem. B* 2006, 110, 8535-8539 have been shown to have tunable C/O ratios ranging from 10 to 500. The term "graphene" as used herein should be understood to include both pure graphene and graphene with small amounts of graphene oxide, as is the case with these materials.

[0014] Further, while graphene is generally described as a one-atom-thick planar sheet densely packed in a honeycomb crystal lattice, these one-atom-thick planar sheets are typically produced as part of an amalgamation of materials, often including materials with defects in the crystal lattice. For example, pentagonal and heptagonal cells constitute defects. If an isolated pentagonal cell is present, then the plane warps into a cone shape. Likewise, an isolated heptagon causes the sheet to become saddle-shaped. When producing graphene by known methods, these and other defects are typically present.

[0015] The IUPAC compendium of technology states: "previously, descriptions such as graphite layers, carbon layers, or carbon sheets have been used for the term graphene . . . it is not correct to use for a single layer a term which includes the term graphite, which would imply a three-dimensional structure. The term graphene should be used only when the reactions, structural relations or other properties of individual layers are discussed". Accordingly, while it should be understood that while the terms "graphene" and "graphene layer" as used in the present invention refers only to materials that contain at least some individual layers of single layer sheets, the terms "graphene" and "graphene layer" as used herein should therefore be understood to also include materials where these single layer sheets are present as a part of materials that may additionally include graphite layers, carbon layers, and carbon sheets.

[0016] Traditionally conductive graphene sheets have produced by mechanical exfoliation. By nature the graphite surface is hydrophobic. Oxidation of graphite followed by exfoliation has been shown to produce more soluble graphene oxide, but with a lower conductivity. Reduction of graphene oxides to increase the conductivity significantly reduces the solubility (<0.5 mg/mL) and makes the material vulnerable to irreversible aggregation.

[0017] Following the research from carbon nanotubes, two main methods to improve surface properties of graphene have been investigated. The first approach is through surface functionalization of reduced graphene oxides in order to make soluble and stable graphene possible for materials process. For example, functional groups (e.g., —CH_3, —SO_3 group) are covalently attached to graphene surfaces through oxygen functionality (—O—, —COOH), but this process also incorporates defects on sp^2 conjugation of carbon atoms, which affect the intrinsic unique properties such as high conductivity.

[0018] The second approach is non-covalent functionalization using surfactant, polymer or aromatic molecules. In general a good electrode material needs to meet some key requirements: good wetting for the electrolyte or catalyst, a good conductive pathway throughout the electrode materials, and a continuous porous network for rapid diffusion and mass transport. To date, efforts to produce materials using the second approach have not approached the theoretical properties of graphene based materials. The present invention overcomes those shortcomings.

SUMMARY OF THE INVENTION

[0019] One aspect of the present invention is thus a nanocomposite material formed of graphene and a mesoporous metal oxide. Preliminary studies of the materials of the present invention have demonstrated that the specific capacity of these nanocomposite materials can be increased to more than 200 F/g. The present invention thus provides nanocomposite materials that exhibit properties heretofore unavailable using materials known in the art. While not limited to such applications, the present invention finds particular utility when employed in supercapacitor applications. The present invention further provides a method for making these nanocomposite materials.

[0020] The method of the present invention general proceeds by first forming a mixture of graphene, a surfactant, and a metal oxide precursor. The metal oxide precursor with the surfactant is the precipitated from the mixture to form a mesoporous metal oxide. The mesoporous metal oxide is then deposited onto a surface of the graphene.

[0021] Preferably, but not meant to be limiting, the surfactant is non-ionic surfactant. A suitable non-ionic surfactant includes, but is not limited to, a tri-block copolymer. Preferably, but not meant to be limiting, the method of making the nanocomposite materials may further include the step of heating the mixture at a temperature of between about 100 to 500 degrees C. to condense the metal oxide on the surface of the graphene.

[0022] Also preferably, but not meant to be limiting, the method of the present invention may further practice the step of heating the mixture from 100 to 500 degrees C. to remove the surfactant.

[0023] The present invention further encompasses a nanocomposite material comprising a mesoporous metal oxide bonded to at least one graphene layer. The nanocomposite material may include embodiments where the mesoporous metal oxide is substantially inert and substantially nonconductive. One example of a suitable mesoporous metal oxide is silica. Preferably, but not meant to be limiting, the graphene layers and the mesoporous metal oxides are generally uniformly distributed throughout the nanoarchitecture of the nanocomposite material of the present invention.

[0024] Preferably, but not meant to be limiting, the mesoporous metal oxide has pore sizes ranging from about 1 nm to about 30 nm. Also preferably, but not meant to be limiting, at least a portion of the mesoporous metal oxide has a thickness between 0.5 and 50 nm and more preferably a thickness between 2 and 10 nm.

[0025] While not meant to be limiting, the present invention provides particular utility when configured as an energy storage device. One suitable energy storage device that takes

advantage of the present invention's unique properties is a configuration wherein a nanocomposite material having mesoporous silica bonded to at least one graphene layer and is utilized as an ultracapacitor. In this configuration, it is preferred that the capacitance of the ultracapacitor is greater than 150 F/g and more preferred that the capacitance of the ultracapacitor is greater than 200 F/g. The ultracapacitor may further be a double layer ultracapacitor.

BRIEF DESCRIPTION OF THE DRAWINGS

[0026] The following detailed description of the embodiments of the invention will be more readily understood when taken in conjunction with the following drawings.

[0027] FIG. **1***a-j* are a series of TEM images of FGS (functionalized graphene sheets) and FGS-MS (functionalized graphene sheet—mesoporous silica) nanocomposites. (a-b) FGS. (c) Cross-section TEM image of FGS. The arrow indicates a region of multilayer FGS on edge. (d) Low magnification plan view of the FGS-MS nanocomposite. (e) Cross-section TEM image of FGS-MS nanocomposite. (f) A high magnification cross-section image showing an ordered mesoporous domain on FGSs. (g-h) High resolution cross-section image near edge of FGS-MS. Arrows show mesoporous silica and graphene layers. (i j)High magnification cross-section image of FGS-MS nanocomposite showing disordeded (i) and ordered (j) mesoporous silica.

[0028] FIG. **2** shows cyclic voltammograms (CV) of FGS and FGS-MS measured in 1M Na_2SO_4 aqueous solution at various scan rates through a potential range of (−1) −0V with saturated Ag/AgCl as the reference electrode. a) CV of FGS and FGS-MS with scan rate of 2 mV/s, (b) CV of FGS and FGS-MS with scan rate of 500 mV/s.

[0029] FIG. **3** is a graph showing the cycling performance of FGS and. FGS-MS. The scan rate is 100 mV/s between (−1) to 0V in a 1M Na_2SO_4 electrolyte.

[0030] FIG. **4** is a graph showing a comparison of the specific capacitances for FGS and all FGS-MS nanocomposites. (a) The specific capacitance at different scan rates in a potential range of (−1)−0 V.

[0031] FIG. **5***a* through d are TEM and electrochemical characterization of Pt-FGS (platinum-functionalized graphene sheet) and Pt-FGS-MS (platinum-functionalized graphene sheet-mesoporous silica) nanocomposites. (a) TEM image of Pt-FGS. (b) TEM image of Pt-FGS-MS. Corresponding insets show dark-field TEM images in a and b. FIG. **5***c* are a cyclic voltammograms for a commercial catalyst (Etek), Pt-FGS and Pt-FGS-MS. FIG. **5***d* is a graph showing a comparison of measured ESA (electrochemically active surface area) in Etek, Pt-FGS and Pt-FGS-MS.

DETAILED DESCRIPTION OF THE PREFERRED EMBODIMENTS

[0032] For the purposes of promoting an understanding of the principles of the invention, reference will now be made to the embodiments illustrated in the drawings and specific language will be used to describe the same. It will nevertheless be understood that no limitations of the inventive scope is thereby intended, as the scope of this invention should be evaluated with reference to the claims appended hereto. Alterations and further modifications in the illustrated devices, and such further applications of the principles of the invention as illustrated herein are contemplated as would normally occur to one skilled in the art to which the invention relates.

[0033] A series of experiments were conducted to demonstrate several aspects of the present invention. One such aspect was the demonstration of a one-step, self-assembly approach to preparing functionalized graphene-mesoporous silica nanocomposites by coating the graphene sheets with a thin layer of mesoporous silica. Another aspect of the present invention was the investigation of the electrochemical applications of these new nanocomposite materials.

[0034] These experiments demonstrated that the combination of mesoporous silica and graphene has the potential to significantly improve electrochemical performance of devices using these nanocomposite materials. For example, but not meant to be limiting, these experiments further investigated the application of the nanocomposites for electrochemical double layer capacitors (supereapacitors). It was shown that coating the conductive graphene with a non-conducting silica material greatly enhanced the electrochemical energy storage capabilities. The specific capacitance of the nanocomposites was more than doubled as compared to that of pure graphene. The increased electrochemical energy storage is attributed to the modification of the graphene surface by mesoporous silica.

[0035] In addition to the use as supercapacitors, the nanocomposite materials of the present invention could also be used for other applications, for example, but not meant to be limiting, as high surface area supports for Pt catalysts in proton exchange membrane fuel cell (PEMFC) applications. Preliminary results of the experiments conducted to demonstrate the present invention suggest that the nanocomposite produces a much higher electrochemically active surface area (ESA) for the Pt particles as compared to both pure graphene and commercial materials, suggesting better dispersion of the catalyst on the composites.

[0036] Those having ordinary skill in the art and the benefit of this disclosure will thus recognize that the method and nanocomposite materials described herein can applied to other mesoporous materials as well as carbon materials beyond graphene for a variety of electrochemical applications.

[0037] Functional graphene sheets (FGSs), a highly conductive graphene from a rapid thermal expansion of graphite oxides, were used in these experiments. To prepare FGS-mesoporous silica (FGS-MS) nanocomposites, FGS was dispersed in a surfactant/silicate sol solution followed by vacuum filtration. The coating of mesoporous silica layer on FGSs is driven by evaporation induced self-assembly. By coating a thin layer of mesoporous silica on the graphene, the intrinsic high conductivity of graphene is maintained, while new function from the inorganic mesoporous silica is introduced.

[0038] 0.125 g poly(ethylene oxide)-b-poly(propylene oxide)-b-poly(ethylene oxide) triblock copolymer (Pluronic P123, $EO_{20}PO_{70}EO_{20}$, Sigma-Aldrich, USA), 0.5 ml tetraethyl orthosilicate (TEOS, Sigma-Aldrich), and 0.4 g 0.1 M HCl were dissolved in 5 ml ethanol. The sol was stirred for 30 mins. 0.01 g FGS was added into the sol followed by vigorous stirring for 15 min. The mixture was dropwise added to a membrane filter under vacuum. The obtained black powders were dried overnight followed by calcination in static air at 400° C. for 2 h with a ramping rate of 1° C./min.

[0039] The electrochemical capacitor performance of FGS and FGS-MS were analyzed with a CHI 660c electrochemical workstation (DH Instruments Inc, Austin, Tex.). All experiments were carried out with a conventional three-electrode

configuration in a beaker-type cell. To prepare the working electrode, 5 mg powder of FGS or FGS-MS powder was dispersed in 1 ml dimethyl formamide or 1 ml H_2O, respectively. The mixtures were sonicated for 5 minutes. 5 μl of the solution was deposited on glassy carbon electrode and dried in air. 5 μl of a 5% Nafion solution was dropped on the top of the electrode to prevent the loss of the composite material. A platinum wire and an Ag/AgCl electrode were used as the counter and reference electrodes, respectively. The electrolyte was 1M Na_2SO_4 aqueous solution. The specific capacitance was calculated from cyclic voltammograms according to C=I/(m×scan rate), where I represents average current in either positive or negative scan, and m is the mass of single electrode. It is well known that due to the series connection of two electrodes in real capacitors, the real capacitor would operate with a capacitance one-fourth that of the single electrode.

[0040] Typical transmission electron microscopy (TEM) images of FGS and FGS-MS nanocomposites are shown in FIG. **1**. FIG. **1***a* shows that the free-standing 2D graphene sheets are not perfectly flat. They display intrinsic microscopic roughening and surface out-of-plane defolinations (wrinkles). Interconnected pocket structures in the cross-sectional TEM image are shown in FIG. **1***b*, with the pocket sizes ranging from 100 to 200 nm. In these nanocomposites, mesoporous silica coating is observed throughout the sample. From high magnification scanning electron microscopy, it is shown that the graphene sheets form open stacked-card structures after the silica coating. No precipitates or separate silica particles are observed from the SEM images. However, TEM images in FIGS. **1***d* to **1***j* clearly show silica mesostructures formed on the FGS surface after the surfactant was removed during calcination.

[0041] In FIG. **1***d*, the underlying graphene morphology is still clearly visible and similar to FIG. **1***a*, but a layer of won't like features covers the entire graphene surfaces. In most of the areas disordered worm-like structures are observed. Cross-sectional TEM images (FIG. **1***e*) show that the disordered mesoporous regions are divided into pockets (domains) by layers of graphene sheets. The pocket structure is similar to what is observed in pure graphene (FIG. **1***b*). Partially ordered mesostructures are only visible in some regions (FIG. **1***f*).

[0042] High resolution TEM images show the interfacial regions between the silica and graphene. FIG. **1***g* shows a very thin layer of graphene sheets. The curved graphene sheets are covered by mesopsorus silica layers closely follow the contours of the graphene sheets. The pore channels separating the silica can be also observed. FIG. **1***h* shows another high resolution image in which both the graphene layers and the nanoporous silica channels can be observed. Like the pure graphene materials, stacked graphene sheets are still observed in the nanocomposites. In high-magnification cross-sectional images shown in FIG. **1***h*, each layer may not represent a single graphene sheet. In cross-sectional TEM, both the underlying graphene and the mesopore structures can be clearly identified near the edge of FGSs. 4 to 7 layers of porous micellar mesostructures (about 40 nm in thickness) indicated by arrows can be observed in mesoporous silica layers on FGS.

[0043] The nitrogen adsorption isotherm further confirmed the existence of mesoporous structure in FGS-MS nanocomposites. Pore size distributions determined using the Barrett-Joyner-Halenda (BJH) model indicate a narrow mesopore of 4 to 5 nm in diameter. This pore size is slightly smaller than the bulk mesoporous materials using the same surfactant due to the shrinkage of planar coating.

[0044] To investigate the effects of coating thickness, solutions with various concentrations of surfactant and TEOS were used to obtain FGS-MS nanocomposites with different coating morphology. Two control samples, FGS-MS-1 and FGS-MS-2, were denoted to the one prepared with surfactant and TEOS concentration 10 times diluted or 5 times higher than typical FGS-MS nanocomposites, respectively as shown in Table 1.

TABLE 1

Synthesis condition of FGS-MS nanocomposite.

	P123 (g)	TEOS (ml)	0.1MHCl (g)	Ethanol (ml)	FGS (g)	Content of silica (wt %)
FGS-MS	0.125	0.5	0.4	5	0.01	29.08
FGS-MS-1	0.0125	0.05	0.4	5	0.01	19.06
FGS-MS-2	0.625	2.5	0.4	5	0.01	80.16

[0045] With a high surfactant and silica concentration, partially ordered mesoporous structures were observed in large areas in FGS-MS-2 (FIG. **1***f*). When a much diluted silica sol was used in the preparation of FGS-MS-1, the mesostructures could be barely observed, but composition analysis clearly reveals the existence of the silica coating.

[0046] The FGS-MS nanocomposites, combining high conductivity of graphene and hydrophilic surface of mesoporous silica, are evaluated as electrodes for electrochemical charge storage in capacitors and compared with FGS. The cyclic voltammograms (CV) of FGSs and FGS-MS nanocomposites recorded at a various scan rates in 1M Na_2SO_4 solutions are shown in FIG. **2**. Both FGS and FGS-MS nanocomposites display a capacitive charging current at both scanning directions across the potential range −1.0 to 0 V (vs. saturated Ag/AgCl reference electrode). CVs of FGS keep ideal rectangular shape at high potential scan rate of 500 mV/s (FIG. **2***b*). A small redox current peak near −0.2V is observed, which comes from reactions of electroactive surface functinoal groups of graphene (e.g., —C—OH, —C═O and —COOH). The single electrode capacitance of FGS, calculated by integrating half of the CV square shapes, is 56 F/g and 39 F/g at scant rate of 2 mV/s and 500 mV/s, respectively.

[0047] The capacitance under the slow scan rate is similar to what is obtained for graphene using two electrode configuration and full cycle integration, which caused a factor of two differences. Normalized against the surface area (600 m^2/g) for the graphene used, a specific capacitance of 10 $\mu F/cm^2$ is obtained, in good agreement with other carbon materials.

[0048] The CV of FGS-MS nanocomposites also show ideal rectangularity at both low and high scan rates (FIGS. **2***a* and **2***b*), but the CV windows of FGS-MS arc much larger than that of FGS, resulting in a much higher capacitance. Cyclic voltammograms clearly show that the coating of mesoporous silica doesn't sacrifice the electrochemical capacitance of graphene but greatly improves its performance. The capacitance of FGS-MS more than doubled to 120 F/g and 95 F/g at scan rate of 2 mV/s and 500 mV/s, respectively. It should be noted that this particular sample contains roughly 30 wt % non-conducting silica measured from thermogravimetric analysis (TGA).

[0049] In principle, the silica should not be expected to contribute to the total capacitance. The specific capacitance

includes the "dead weight" of the silica phase. If the weight of the silica were not included in the calculation, the specific capacitance of graphene in the nanocomposites should be even higher, 171 F/g and 136 F/g (of graphene) at scan rate of 2 mV/s and 500 mV/s, respectively. The specific capacitance then corresponds to 28 $\mu F/cm^2$, which is high for carbon materials.

[0050] The cycling performance of FGS and FGS-MS are presented in FIG. **3**. Both FGS and FGS-MS show good stability for at least 1000 cycles with capacitance loss within 15%. The gradual decrease in capacitance may result from pseudocapacitance contributed from redox reactions of surface functional groups of graphene, similar to previous observation in functionalized carbon nanotubes.

[0051] FIG. **4** summarizes the capacitance of FGS and all FGS-MS samples at different scan rates. As shown in FIG. **4***a*, capacitances slightly decrease with increasing scan rate in all samples. With addition of a mesoporous silica coating, the capacitance of FGS-MS nanocomposites significantly increases and doubles the capacitance of pure FGS over the entire scan rate range. It should be noted that much higher silica content in FGS-MS-2 causes the capacitance to decrease to below the level for pure FGS, which may be attributed to decreased conductivity and the increase of dead weight with excessive silica coating. Another important observation is that the enhancement in electrochemical capacitance depends on the bias. Although FGS-MS nanocomposites have a much higher specific capacitance under both positive (0 to 1 V) and negative bias (−1 to 0V), the results under negative bias are much more obvious (scan rate of 100 mV/s). Under negative bias, FGS-MS and FGS-MS-1 exhibit 2.4 times and 1.8 times enhancement over FGS respectively, but under positive bias, FGS-MS and FGS-MS-1 only exhibit 1.9 times and 1.2 times enhancement.

[0052] The above discussion confirms that the mesoporous silica coating amplifies the electrochemical response of the carbonaceous material. Furthermore, from all the CV curves, the open circuit potential remains the same, suggesting that there is no additional redox reaction in the nanocomposite. Traditionally redox materials are applied to carbon to increase the capacitance. There has been no study on using "inert, nonconductive" silica as the coating materials. There might be several reasons for the observed enhanced capacitance. First, since the graphene is hydrophobic and the preparation of the nanocomposite involves the use of a surfactant and hydrophilic silica, it is possible the graphene materials become more dispersed and the mesoporous silica prevents the graphene sheets from restacking due to van der Waals forces. Although the overall microstructural characterization by TEM and SEM does not reveal significant changes, the specific surface area measured by nitrogen absorption (BET method) is indeed increased from 600 m^2/g to 800 m^2/g. Since it is well known the mesoporous silica prepared using the current method has an approximate surface area of 450 m^2/g, the increase of the surface area can be only attributed to better separation of the graphene sheets. However, this surface area increase of approximately 30% is not sufficient to explain the more than 100% increase in the specific capacitance. Therefore, surface chemistry in addition to surface area, must play an important role.

[0053] The hydophilic mesoporous silica with continuous pore channels could improve wetting and diffusion. Generally, higher surface area of carbon leads to higher ability for charge accumulation, and thus the higher specific capacitance. However, specific capacitances obtained from carbon materials are usually much lower than expected. One main cause of the lower capacitance than expected is poor wettability of the electrode material in electrolyte solution, which results in a less accessible surface area for the formation of electrochemical double layers.

[0054] In the case of FGSs, the surface of FGSs is relatively hydrophobic after high temperature process during thermal expansion, resulting in poor wettability. In principle, the specific capacitance of graphene can be significantly increased if much of the intrinsic surfaces can be accessed. After functionalization with mesoporous silica, the FGS-MS nanocomposites became hydrophilic. A comparison of FTIR spectra of bare FGS and FGS-MS showed the presence of surface hydroxyl groups in FGS-MS. In addition, the mesoporous silica contains a continuous network of uniform, nanometer-size channels. The improved wetting and the nanoporous channels should have a positive effect on improving the accessibility of the electrolyte to the electrode surfaces, therefore increasing the specific capacitance.

[0055] Another factor to consider is whether the electrochemical double layer of silica itself contributed to the total capacitance. Silica is able to develop a very high negative surface charge and has one of the highest electrical double layer potential and capacitance (over 60 $\mu F/cm^2$). If the interpenetrating network of graphene and silica is viewed as an equivalent circuit of two capacitors, the contribution from silica can be estimated based on the area specific capacitance (60 $\mu F/cm'$), the weight percentage (30 wt % for example) and the specific surface (about 450 m^2/g for evaporation driven self-assembly). The contribution from silica becomes 80 F for 0.3 g silica. The contribution from graphene is 40 F for 0.7 g graphene. Then the total specific capacitance is 120 F/g for the 30 wt % silica sample (FGS-MS), which is almost the same as the experimental results. A similar calculation for the 20 wt % silica sample (FGS-MS-1) can be performed, which gives an estimated specific capacitance of 100 F/g, again in excellent agreement with the experimental result.

[0056] These calculations suggest that the increased capacitance is likely derived from the double layer capacitance of silica. From the TEM images, the total silica coatings thickness are approximately 40 nm, and each individual layer in the high resolution TEM images is only a few nanometers.

[0057] FGS-MS nanocomposites can also be used as a novel electrode support for electrochemical catalysis. In Polymer Electrolyte Membrane fuel cells (PEMFCs), the electrooxidation of hydrogen or methanol directly converts chemical energy into electricity. PEMFCs are attractive for transportation vehicles and small-scale static power supplies because of their high theoretical efficiency. A typical hydrogen or methanol fuel cell consists of an anode and a cathode that are separated by the electrolyte. The anodic oxidation reactions in hydrogen and methanol fuel cells produce protons and electrons. The cathodic reactions in both types of fuel cells involve the reduction of O_2 to produce OH^-, which combines with H^+ to produce water to complete the overall electrochemical reactions. Currently the leading cathode electrocatalysts are carbon supported platinum (Pt) and Pt-based alloys. Despite its enormous potential, the PEMFC technology is not widely used at present, partially due to the cost of the Pt containing cathodes. Therefore one of the major challenges in the commercialization of fuel cells is to substantially reduce the metal loading of the Pt electrocatalysts. One approach to accomplish this goal to develop better cath-

ode supports for improved dispersion and adhesion of the Pt catalysts. In the literature, aero-gel silica-carbon was investigated to support Pt and it was found that the addition of aero-gel silica significantly increased the activity of the catalyst.

[0058] The main advantage of graphene is its high surface area, good crystallinity and good conductivity, but its performance as a cathode material for Pt catalyst has not been investigated. In this study, Pt nanoparticles are loaded onto FGS and FGS-MS nanocomposites (denoted to Pt-FGS and Pt-FGS-MS, respectively) via impregnation methods to investigate its electrochemical surface area (ESA), which is an indication of the dispersion and the activity of the metal catalyst particles. The ESA value is determined by the particle sizes and the accessible surfaces. A higher ESA value suggests a smaller particle size, and higher catalytic activity.

[0059] FIGS. **5***a* and **5***b* show TEM images of as-prepared Pt-FGS and Pt-FGS-MS, respectively. TEM images show uniform, even distribution of Pt nanoparticles on FGS and FGS-MS substrates. Dark-field TEM images in insets show crystalline Pt nanoparticles on FGS and FGS-MS. The average size of the Pt nanoparticles on Pt-FGS is around 2.0 nm which is larger than that (1.6 nm) on FGS-MS. Pt nanoparticle size on both Pt-FGS and Pt-FGS-MS is much smaller than that of commercial electrocatalyst Etek, which is still one of the best cathode materials for PEMFCs with Pt supported on high surface area carbon. FGS has a surface area of 600 m^2/g and after coating with silica, FGS-MS still possess surface areas as high as 800 m^2/g which is much higher than that of commercial Etek (250 m^2/g). Cyclic voltammograms (FIG. **5***c*) in 0.5M H_2SO_4 show standard hydrogen adsorption behavior with potential at 0.12 and 0.23 V. Consistent with above mentioned capacitor study, Pt-FGS-MS also shows much higher capacitance charge storage than Pt-FGS in the potential range in H_2SO_4 solution. The ESA is estimated from the peak area in the CV curve from 0.12 to 0.23 V. The Etek has an electrochemically active surface area (ESA) of 60 m^2/g in our test. For graphene, the ESA value increases to 65 m^2/g (Pt-FGS) and Pt-FGS-MS is 85 m^2/g as shown in FIG. **5***d*. Both graphene-containing samples show higher ESA than that of the commercial Etek. For a given quantity of Pt, the smaller the metal nanoparticle size, the higher the electrochemically active surface area. The higher ESA of Pt obtained from FGS and FGS-MS may be attributed to the smaller Pt nanoparticles deposited.

[0060] One difference between graphene and Etek is that the former has a much higher surface area, which might have contributed to a higher ESA for native graphene, The mesoporous silica coating on graphene further increased the active surface area. The silica surface maybe helpful in improving the wetting and the adhesion between the metal particles and the carbon surfaces, which is a significant problem in PEMFCs,

[0061] In summary, these experiments demonstrated a novel and effective method to functionalize a graphene surface by coating graphene sheets with a thin layer of mesoporous silica in a one step self-assembly process. These nanocomposite materials showed surprising improvement in electrochemical energy storage capabilities as compared to pure graphene. The specific capacitance increases from about 55 F/g of bare graphene to more than 120 F/g of the nanocomposites. Pt nanoparticles loaded on the functionalized graphene-mesoporous silica nanocomposites also showed much higher electrochemical surface area than that of pure graphene sheets. This disclosure thus provides those having ordinary skill in the art the ability to functionalize and process not only graphene, but also other materials for electrochemical applications. Those having ordinary skill and the benefit of this disclosure will readily recognize that with the rich silane chemistry, various functional groups can be grafted on the mesoporous silica layer. In this manner, many other applications, including but not limited to sensors, nanocomposites, membranes and catalysts supports, are thereby enabled by this disclosure.

[0062] While the invention has been illustrated and described in detail in the drawings and foregoing description, the same is to be considered as illustrative and not restrictive in character. Only certain embodiments have been shown and described, and all changes, equivalents, and modifications that come within the spirit of the invention described herein are desired to be protected. Any experiments, experimental examples, or experimental results provided herein are intended to be illustrative of the present invention and should not be considered limiting or restrictive with regard to the invention scope. Further, any theory, mechanism of operation, proof, or finding stated herein is meant to further enhance understanding of the present invention and is not intended to limit the present invention in any way to such theory, mechanism of operation, proof, or finding.

[0063] Thus, the specifics of this description and the attached drawings should not be interpreted to limit the scope of this invention to the specifics thereof. Rather, the scope of this invention should be evaluated with reference to the claims appended hereto. In reading the claims it is intended that when words such as "a", "an", "at least one", and "at least a portion" are used there is no intention to limit the claims to only one item unless specifically stated to the contrary in the claims. Further, when the language "at least a portion" and/or "a portion" is used, the claims may include a portion and/or the entire items unless specifically stated to the contrary. Likewise, where the term "input" or "output" is used in connection with an electric device or fluid processing unit, it should be understood to comprehend singular or plural and one or more signal channels or fluid lines as appropriate in the context. Finally, all publications, patents, and patent applications cited in this specification are herein incorporated by reference to the extent not inconsistent with the present disclosure as if each were specifically and individually indicated to be incorporated by reference and set forth in its entirety herein.

1. A method comprising:

providing graphene;

mixing the graphene with a surfactant and a metal oxide precursor;

precipitating the metal oxide precursor with the surfactant to form a mesoporous metal oxide; and

depositing the mesoporous metal oxide onto surfaces of the graphene;

forming a nanocomposite material with the mesoporous metal oxide bonded directly to the surfaces of the graphene.

2. The method of claim **1** wherein the graphene comprises functionalized graphene sheets prepared by thermal expansion of graphite oxide.

3. The method of claim **1** further comprising dispersing the graphene in the surfactant to yield dispersed graphene layers

comprising 1 to 127 graphene sheets, and bonding the mesoporous metal oxide directly to the surfaces of the graphene layers.

4. The method of claim **1** wherein the surfactant is a non-ionic surfactant,

5. The method of claim **1** wherein the non-ionic surfactant is a tri-block copolymer.

6. The method of claim **1** wherein the forming of the nanocomposite material with the mesoporous metal oxide bonded directly to the surfaces of the graphene comprises heating the mixture from 100 to 500° C. to condense the mesoporous metal oxide on the surfaces of the graphene.

7. The method of claim **1** wherein the mesoporous metal oxide of the nanocomposite material has pores ranging in size from about 1 nm to about 30 nm.

8. The method of claim **1** wherein the mesoporous metal oxide of the nanocomposite material has a thickness ranging from about 0.5 nm to about 50 nm.

9. The method of claim **1** further comprising dispersing the graphene in the surfactant prior to mixing the graphene with the metal oxide precursor.

10. The method of claim **3** further comprising forming the nanocomposite material into open stacked-card structures of the multiple graphene layers coated with mesoporous metal oxide.

11. The method of claim **1** wherein the metal oxide comprises silica.

12. The method of claim **1** further comprising generally uniformly distributing the graphene and mesoporous metal oxide throughout the nanocomposite material.

* * * * *